Cell Reports
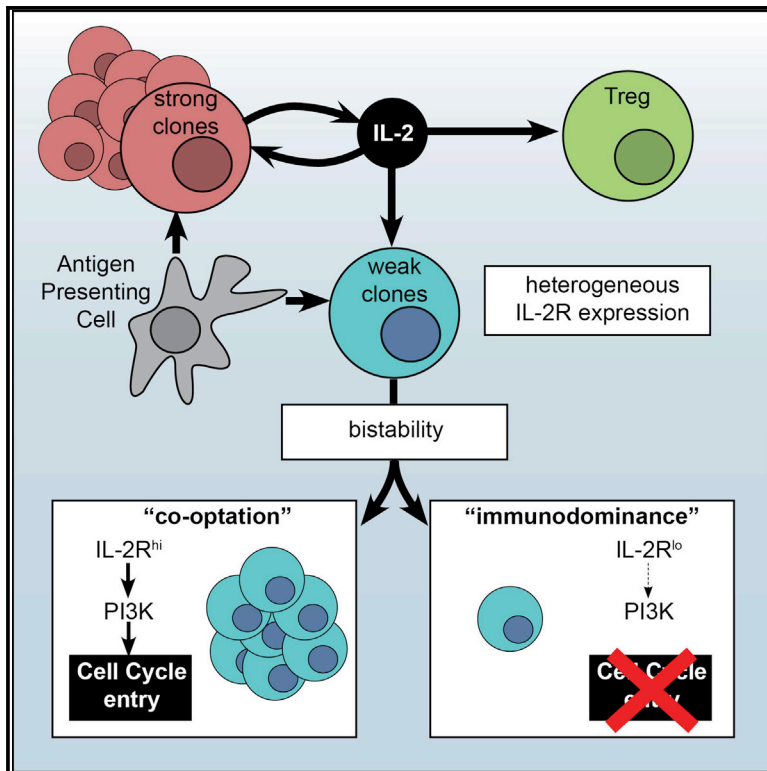
T Cells Integrate Local and Global Cues to Discriminate between Structurally Similar Antigens

Graphical Abstract

Authors

Guillaume Voisinne, Briana G. Nixon, ..., Massimo Vergassola, Grégoire Altan-Bonnet

Correspondence

altanbog@mskcc.org

In Brief

T cells integrate a wealth of signals to discriminate between structurally related antigens. Voisinne et al. demonstrate how IL-2, generated by neighboring strongly activated T cell clones, induces weaker clones to proliferate through the activation of PI3K, thus highlighting the collective nature of antigen discrimination by T cells.

Highlights

- Strongly activated T cell clones induce weaker clones to proliferate through IL-2

- IL-2-induced PI3K activation mediates the co-optation of weak T cell clones

- A quantitative model shows how antigen and IL-2 signal additively to activate T cells

- Co-optation is set by cell number, antigen load, and competition with T-reg cells

CellPress

T Cells Integrate Local and Global Cues to Discriminate between Structurally Similar Antigens

Guillaume Voisinne,[1,2,4] Briana G. Nixon,[3] Anna Melbinger,[6] Georg Gasteiger,[3,5] Massimo Vergassola,[6] and Grégoire Altan-Bonnet[1,2,3,*]

[1]Center for Cancer Systems Biology, Memorial Sloan Kettering Cancer Center, New York, NY 10065, USA
[2]Program in Computational Biology, Memorial Sloan Kettering Cancer Center, New York, NY 10065, USA
[3]Program in Immunology, Memorial Sloan Kettering Cancer Center, New York, NY 10065, USA
[4]Centre d'Immunologie de Marseille-Luminy, UM2 Aix-Marseille Université, Inserm U1104, CNRS UMR7280, Marseille 13288, France
[5]Institute of Medical Microbiology and Hygiene, University of Mainz Medical Center, Mainz 55131, Germany
[6]Department of Physics, University of California San Diego, La Jolla, CA 92093, USA
*Correspondence: altanbog@mskcc.org
http://dx.doi.org/10.1016/j.celrep.2015.04.051

SUMMARY

T lymphocytes' ability to discriminate between structurally related antigens has been attributed to the unique signaling properties of the T cell receptor. However, recent studies have suggested that the output of this discrimination process is conditioned by environmental cues. Here, we demonstrate how the IL-2 cytokine, collectively generated by strongly activated T cell clones, can induce weaker T cell clones to proliferate. We identify the PI3K pathway as being critical for integrating the antigen and cytokine responses and for controlling cell-cycle entry. We build a hybrid stochastic/deterministic computational model that accounts for such signal synergism and demonstrates quantitatively how T cells tune their cell-cycle entry according to environmental cytokine cues. Our findings indicate that antigen discrimination by T cells is not solely an intrinsic cellular property but rather a product of integration of multiple cues, including local cues such as antigen quality and quantity, to global ones like the extracellular concentration of inflammatory cytokines.

INTRODUCTION

Self/non-self discrimination by T lymphocytes is a critical function of the adaptive immune system for eradicating pathogen-infected tissues while sparing uninfected tissues. Such discrimination is also at play when T cells rely on their ability to detect "altered self" and eradicate tumors (Houghton and Guevara-Patiño, 2004). Quantitative models of ligand discrimination by T cells dwell on the dynamics of signal transduction (Feinerman et al., 2008a). The premise for these models is the experimental observation that the potency of antigen ligands correlates with the lifetime of their complex with the T cell receptor (TCR). Minute differences in these complex lifetimes—as documented experimentally (Huppa et al., 2010; Liu et al., 2014)—are amplified through kinetic proofreading (McKeithan, 1995), through mechanical sorting (Liu et al., 2014; Qi et al., 2001), or through differential activation of positive/negative feedbacks (Altan-Bonnet and Germain, 2005; François et al., 2013). Ultimately, models of such dynamic sorting of the quality of the antigen/TCR interaction account for the speed, sensitivity, and specificity of T cell activation, with the additional insight about the existence of antagonism by sub-threshold ligands (Altan-Bonnet and Germain, 2005; François et al., 2013) and the origin of phenotypic diversity because of endogenous variability in the abundance of key signaling regulators (Feinerman et al., 2008b).

Antigen discrimination by T cells has been considered mostly as the intrinsic response of individual cells. However, recent studies have demonstrated that the threshold of T cell activation can be modulated (Slifka and Whitton, 2001), in particular when environmental cues are added (McNally et al., 2011; Pipkin et al., 2010; Richer et al., 2013; Williams et al., 2006). Hence, antigen discrimination may not be cell intrinsic per se but rather collectively tunable by cytokines and chemokines produced by neighboring cells (Richer et al., 2013). Such insight would open avenues to manipulate the repertoire of T cell clones responding to an infection or to tumors. A specific example is a study where ablation of the regulatory T cell compartment led to the enlargement of the repertoire of responding cells, recruiting additional clones of weaker affinity for the antigen to the adaptive immune response against infection (Pace et al., 2012). Hence, rather than a set threshold of activation for each T cell (Au-Yeung et al., 2014), integration of environmental cues may lead to fine tuning the response to antigens, raising the possibility that co-responding T cells could modulate each other's responses, either negatively through competition for limited cytokines or chemokines (Busse et al., 2010; Feinerman et al., 2010; Pace et al., 2012) or positively through synergy between antigen and chemokine/cytokine signaling (Pace et al., 2012; Richer et al., 2013)

Here, we explore how the strong antigen response of CD8+ T cells impact the activation of neighboring weaker clones

(a process akin to co-optation in decision making). We demonstrate a critical role for IL-2 as a cytokine whose accumulation and sensing by T cells add to the signaling response of the TCR, enabling full and complete activation despite a sub-threshold response to antigen. Strong activation of few T cell clones generates sufficient IL-2 to co-opt a fraction of weaker clones into activation. We identify cumulative PI3K activation as the dominant molecular mechanism controlling cell-cycle entry through integration of TCR and IL-2 receptor (IL-2R) signals.

To understand quantitatively how IL-2 modulates cell-cycle entry for weakly stimulated cells, we developed an experimentally parametrized computational model of the integration of TCR and IL-2R signals. Such modeling approach has recently provided valuable insights about different functions of the immune system, with theoretical efforts addressing how the TCR signaling machinery achieves ligand discrimination (François et al., 2013; Stepanek et al., 2014), how T cells regulate their differentiation and cell lineage commitment (Buchholz et al., 2013; Gerlach et al., 2013; Schulz et al., 2009), how populations of T cells respond collectively to antigens and cytokines (Hart et al., 2014; Tkach et al., 2014), etc. Computational models of the immune response serve three purposes: (1) testing the sufficiency of our biological understanding; (2) tackling the combinatorial and dynamic complexity of immune regulations; and (3) designing new perturbations for immunotherapeutic manipulations. The strength of these recent modeling efforts resides in their experimental parametrization, enhancing the biological relevance of their results and leading to explicit predictions that can be tested experimentally.

Here, using our model of integration of local TCR and global IL-2R signals, we demonstrate that non-linear signal transduction coupled to the inherent stochasticity of the processes regulating gene expression accounts for the observed heterogeneity of first division times in response to IL-2. We also predict and confirm experimentally how entry into cell cycle is modulated by IL-2 signals and is strongly dependent on antigen affinity and availability. Extending our model to the context of duoclonal populations of T cells, we further predict and experimentally confirm how co-optation of weaker clones depends on cell density and antigen availability. Finally, we investigate how regulatory T cells (T-reg cells) can regulate the co-optation of weaker clones based on their consumption of IL-2 and discuss potential applications for clinical immunotherapies.

RESULTS

Inter-clonal Co-optation among CD8+ T Cells Depends on TCR Signal Strength

To investigate the possible interdependencies within a polyclonal population of T cells, we used two well-characterized CD8+ TCR transgenic T cells, namely the OT-1 and P14 cell clones. Each T cell clone expresses a TCR with high affinity for a specific agonist ligand, a peptide (SIINFEKL, denoted as N4 for OT-1 cells; *KAVYNFATM*, denoted as GP_{33-41} for P14 cells) presented by a particular subset of MHC-I molecule (H-2K^b for N4 and H-2D^b for GP_{33-41}) on the surface of antigen-presenting cells (APCs). We isolated TCR-transgenic T cells from the spleen of naive OT-1 and P14 mice and co-cultured these two T cell

populations in the same wells. To ensure that antigen presentation was minimally affected by the presence of the other cell type, we used distinct sets of APCs to present the ligands specific for each cell type (Figure 1A). We monitored the proliferation of each cell type simultaneously by monitoring with single-cell resolution the dilution of an amine reactive dye (CTV for OT-1 cells and CFSE for P14 cells). This proliferation assay allows one to track the number of divisions a given cell has undergone until the time of observation (Figure 1B). Specifically, we tested a set of altered peptide ligands for OT-1 T cells (Zehn et al., 2009) with varying capacities to stimulate. We observed that, although most of the OT-1 cells (>96%) proliferated when stimulated by the agonist antigen (H-2K^b/N4), only 25% of OT-1 cells divided when they were stimulated by equivalent quantities of the H-2K^b/G4 variant (Figures 1C and 1D). Surprisingly, the percentage of OT-1 cells to proliferate under G4 stimulation increased (to more than 60%) when co-cultured P14 cells were simultaneously activated in the same culture milieu. In contrast, OT-1 cells stimulated by the agonist N4 were largely indifferent to the activation status of the co-cultured P14 cells, with close to 98% of OT-1 cells entering the cell cycle (Figures 1C and 1D). Hence, the vicinity of activated P14 cells could co-opt weakly activated neighboring T cells that would otherwise fail to enter the cell cycle and proliferate.

IL-2 Mediates the Inter-clonal Co-optation of Weakly Stimulated CD8+ T Cells

To investigate the signaling mechanism co-opting weakly stimulated T cells, we repeated the experiments described in Figure 1B and further inhibited JAK kinases (whose activation is critical for the response to extracellular cytokines): we found that JAK inhibition entirely abrogated the co-optation from P14 cells (Figures 1C and 1D). This strongly suggested that soluble factors (i.e., cytokines activating the JAK/STAT pathway) play a major role in this inter-clonal co-optation. We therefore tested directly the impact of different cytokines including IL-2, IL-4, IL-6, IL-7, IL-9, IL-15, IL-21, and IFN-γ on the activation of OT-1 T cells stimulated with the weak agonist G4. We found that, among all the cytokines tested, only IL-2 and IL-4 were able to substantially co-opt weakly stimulated CD8+ T cells and increase the fraction of OT-1 precursor cells that entered cell cycle (Figure 1E). It is important to note here that other cytokines, such as IL-7, maintained cell viability as well as IL-2 and IL-4, but they could not trigger entry into the cell cycle on their own (see Figure S1). Titrations of IL-2 and IL-4 revealed slightly different effects of these cytokines on cycle entry and survival: whereas IL-2 was found to be more efficient in triggering cell-cycle entry, IL-4 could sustain cell viability better than IL-2 (see Figure S1).

We next tested whether the candidate cytokines IL-2 or IL-4 could be responsible for the co-optation of weak T cell clones in co-culture settings. We used antibody blockade to specifically inhibit the effects of IL-2 or IL-4 in the co-culture. We found that, whereas the co-optation of weakly activated OT-1 was unaltered when IL-4 was blocked, IL-2 blockade abrogated this co-optation almost entirely (Figure 1F). We confirmed the importance of IL-2 signaling as a key mediator of the inter-clonal co-optation using a blocking antibody against IL-2Rα, the α subunit of the IL-2R (also named CD25). Other studies suggested that CCL3/4/5
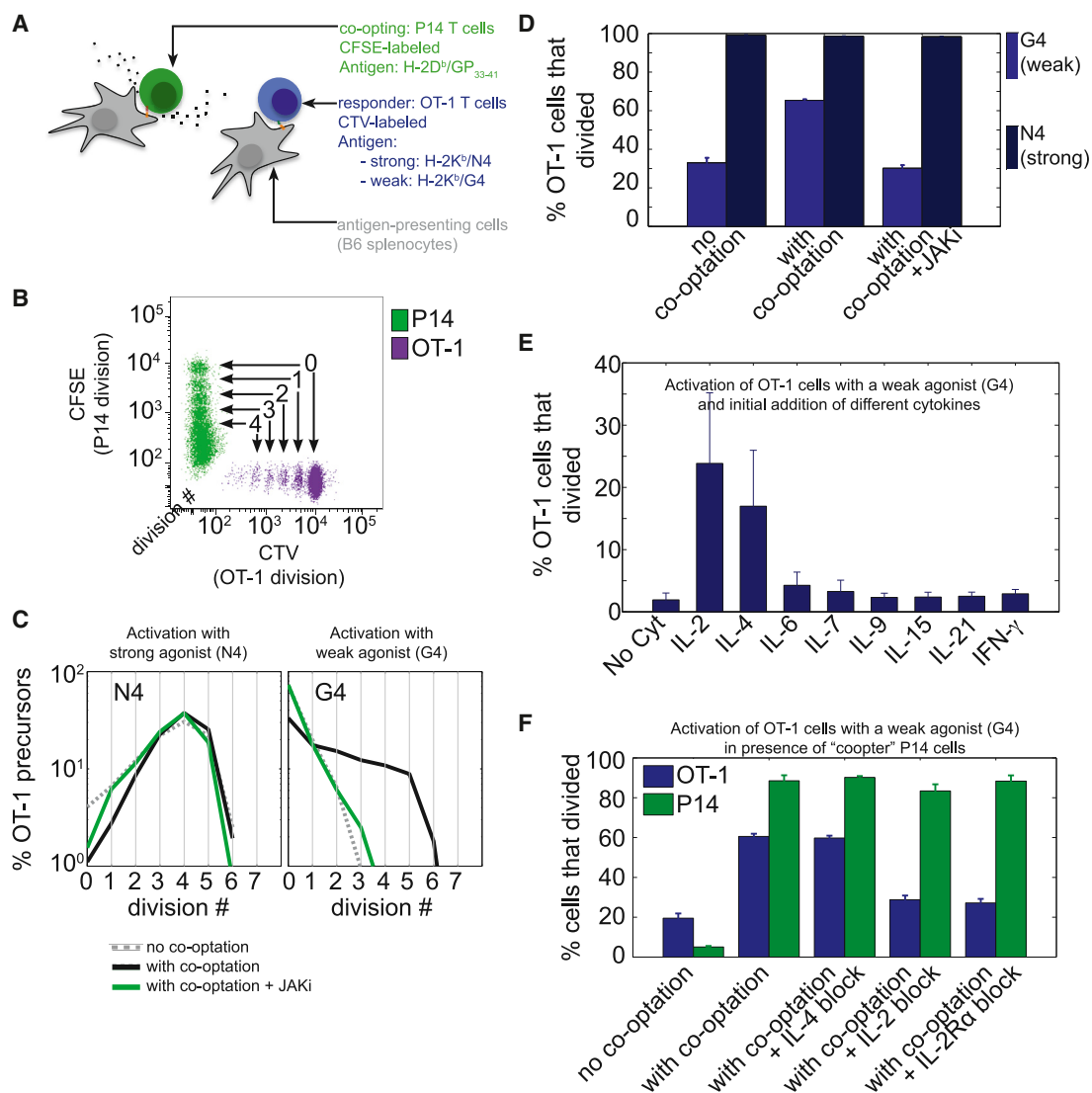
**Figure 1. The Inter-clonal Co-optation of Weakly Activated CD8+ T Cells Is Dependent on IL-2**

(A) Two different TCR transgenic CD8+ T cell populations (P14 and OT-1) were labeled with different amine reactive dyes (CFSE and CTV, respectively) and stimulated in vitro with specific antigens presented by distinct APCs.

(B) Tracking of the proliferation of the two different T cell populations by flow cytometry using the dilution of a fluorescent amine reactive dye (CFSE for P14 cells and CTV for OT-1 cells). We present one representative dot plot of CFSE and CTV MFI for live CD8+ cells after 3 days of co-culture. At each cell division, the amount of the amine reactive dye per cell is divided uniformly by a factor 2 among daughter cells, which allows one to track the number of divisions experienced by a given cell until the time of observation and to estimate the number of divisions performed by precursor cell.

(C and D) Activated P14 cells co-opt only weakly stimulated OT-1 cells, and this is conditioned upon JAK signaling. (C) Distributions of the number of cell divisions per OT-1 precursor cells are measured after 3 days in the in vitro co-culture system presented in (A) and (B). OT-1 cells were stimulated with K^b MHC loaded with either a strong (N4, peptide sequence: SIINFEKL) or a weak agonist (G4, peptide sequence: SIIGFEKL). For each condition of stimulation for the OT-1 cells, the co-cultured P14 cells were either not stimulated ("no co-optation" condition) or stimulated with their cognate antigen GP_{33-41} ("with co-optation" condition) in the presence or absence of a JAK inhibitor (AZD1480; 1 μM). (D) Percentages of OT-1 precursor cells that divided are reported for the experiment shown in (C). Error bars represent mean ± SD for three replicates; the results are representative of n ≥ 3 independent experiments.

(E) Effect of the addition of different cytokines on the proliferation of OT-1 cells stimulated with the weak agonist K^b/G4 in the absence of co-opting P14 cells. A given dose of cytokine (1 nM) was added at time t = 0, and the number of OT-1 precursors that divided was estimated after 3 days. Error bars represent mean ± SD for three replicates; the results are representative of n ≥ 3 independent experiments. Among the cytokines tested, IL-2 and IL-4 were found to be the only ones to allow a significant fraction of weakly stimulated OT-1 cells to proliferate.

(F) IL-2 and not IL-4 is responsible for the co-optation of OT-1 cells by P14 cells. OT-1 cells were stimulated with a weak agonist (K^b/G4) in the presence of P14 cells left either unstimulated (no co-optation) or stimulated by their cognate antigen D^b/GP_{33-41} (with co-optation). Blocking antibodies against mouse IL-2 (clone JES6-1A12) and IL-4 (clone 11B11) were added at time t = 0 to identify the cytokines mediating the co-optation of OT-1 cells. The effect of IL-2 blockade was confirmed using a blocking antibody against the alpha subunit of the IL-2 receptors (CD25; clone PC61.5). Error bars represent mean ± SD for three replicates; the results are representative of n ≥ 3 independent experiments.
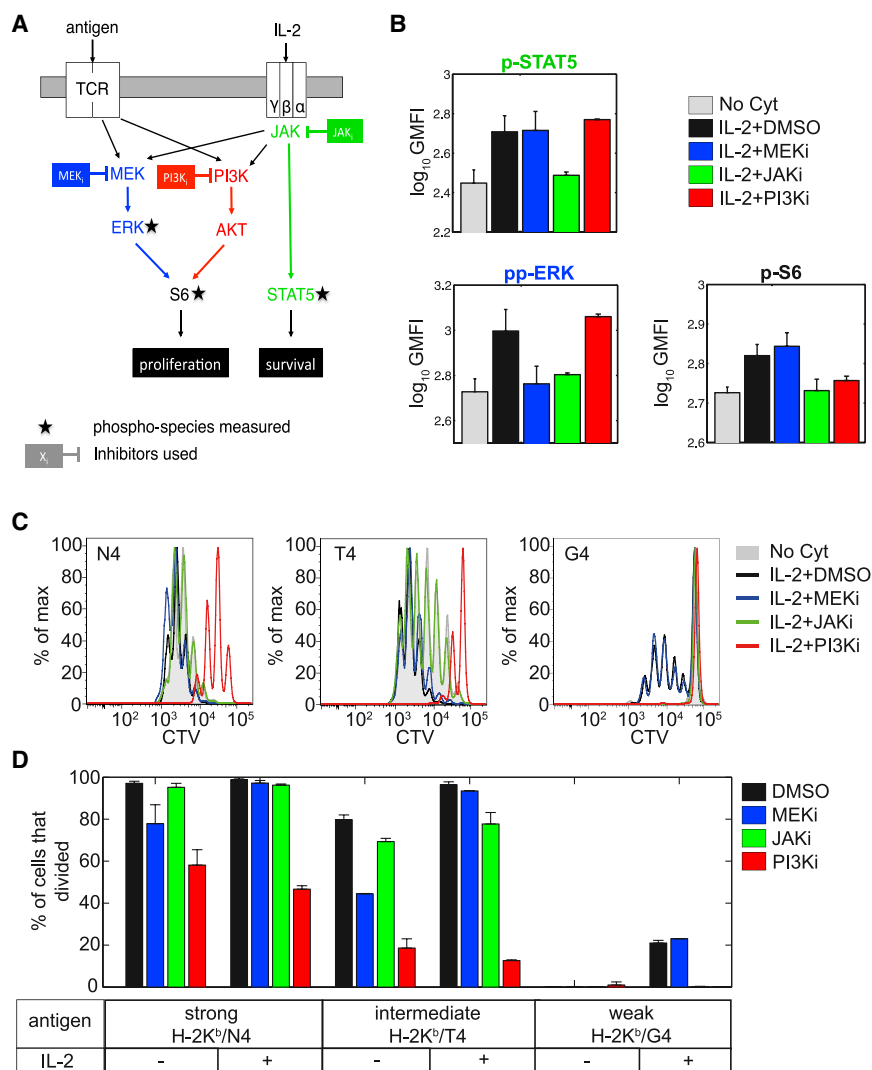
Figure 2. IL-2 Modulation of Cell Cycle Entry Relies on PI3K Activation and Is Independent of MAPK Activity

(A) Schematic representation of the signaling pathways downstream of the TCR and the IL-2R. The different phospho-species measured are indicated by black stars. Inhibitors used here are represented next to their target.

(B) Effect of small-molecule inhibitors on IL-2 signaling. We report the GMFI of the phospho signals indicated in OT-1 T cell blasts left unstimulated or stimulated with 1 nM IL-2 at 37°C for 15 min in the presence of different inhibitors (MEKi, 1 μM; JAKi, 1 μM; PI3Ki, 3 μM). Error bars represent mean ± SD for three replicates; the results are representative of n ≥ 3 independent experiments.

(C and D) Effect of IL-2 and small-molecule inhibitors on the proliferation of OT-1 CD8+ T cells stimulated with antigens of varied strength (N4 > T4 > G4). Cells were cultured for 3 days in the presence of a blocking antibody against the endogenous mouse IL-2 (clone JES6-1A12) either alone ("No Cyt") or with the addition of an initial dose (1 nM) of human IL-2 and different inhibitors (MEKi, 1 μM; JAKi, 1 μM; PI3Ki, 10 μM). We report the histogram of the CTV GMFI (C) and the percentage of OT-1 precursor cells (D) that divided for the experiment shown in (C). Note that, for reasons of readability, histograms corresponding to stimulations in absence of IL-2 and in the presence of inhibitors are not shown in (C). Error bars represent mean ± SD for three replicates; the results are representative of n ≥ 3 independent experiments.

chemokines were possible mediators of the activation of low-affinity clones in vivo (Pace et al., 2012); however, in our experimental in vitro settings, we found that the initial addition of these chemokines could not trigger proliferation of weakly stimulated clones (Figure S1). Moreover, blocking CCL3/4/5 chemokines did not abrogate the co-optation of weakly stimulated clones when co-cultured with strongly stimulated neighboring P14 cells (Figure S1). Therefore, in our experimental in vitro settings, the inter-clonal boost to entrain weak T cell clones into proliferation is mediated by soluble IL-2 secreted by neighboring cells.

We further investigated when IL-2 can synergize with TCR signals to drive cell-cycle entry for T cell responding to weak antigen stimulation. We delayed the addition of IL-2 after the initial stimulation by weak agonists and found that IL-2 is needed in the first 20–30 hr following antigen stimulation (Figure S1). Using IL-7 as a factor promoting survival without triggering cell-cycle entry (see Figures 1E and S1), we demonstrated that the early requirement for IL-2 for cell proliferation was independent of cell death (Figure S1).

To confirm the activation status of weakly stimulated CD8+ T cells in presence of IL-2, we measured the expression of surface activation markers CD44 and CD69, transcription factors Tbet and Eomes, as well as production of IL-2 and IFN-γ and found them comparable to that of strongly stimulated cells proliferating without external IL-2 (Figure S2). Thus, co-optation of weakly stimulated T cells in presence of IL-2 leads to a full and complete activation similar to that of strongly activated cells, albeit at lower frequency. Our results therefore demonstrate that sensing of IL-2 in the first hours following antigen encounter can trigger the complete activation of a fraction of weakly stimulated T cells.

IL-2 Signaling Contributes to Cell Cycle Entry through PI3K Activation

Next, we sought to identify the molecular mechanisms by which IL-2 signaling contributes to cell-cycle entry for weakly activated CD8+ T cells. We first combined the use of small-molecule inhibitors to target several signaling pathways, namely the JAK-STAT, MAPK, and PI3K-AKT-mTOR pathways, downstream of the TCR and IL-2R and measurements of the abundance of phosphorylated species implicated in the activation of these pathways (Figure 2A). Phosphorylation of STAT5 was used as a control for IL-2R stimulation. MEK1/2 and PI3K inhibition did not affect

STAT5 phosphorylation following IL-2R engagement whereas, as expected, it was entirely abrogated by JAK inhibition (Figure 2B). As previously reported (Brennan et al., 1999; Cho et al., 2013), we observed that both S6 ribosomal protein (denoted as S6) and ERK1/2 (noted ERK) were phosphorylated after IL-2 stimulation. Although S6 is reported as a target for activated ERK (Wang et al., 2001), MEK1/2 inhibition did not abrogate IL-2-mediated phosphorylation of S6. Instead, PI3K inhibition efficiently prevented S6 phosphorylation without affecting ERK phosphorylation after IL-2 stimulation (Figure 2B). In line with previous results demonstrating the importance of S6 activation by PI3K in the control of cell-cycle progression (Brennan et al., 1999), our signaling results suggested a critical role for PI3K activation in mediating IL-2 impact on cell-cycle progression in the context of weak TCR stimuli.

To confirm this at the functional level, we used the proliferation assay presented above. We stimulated OT-1 T cells with antigens of different affinities for the TCR (H-2K^b-expressing cells, loaded with N4, T4, and G4 peptides, in descending order of antigenicity) in the presence or absence of IL-2 and inhibition of the pathways under consideration (Figure 2A). CD8+ T cells activated by a TCR agonist produce endogenous IL-2. To ensure a uniform amount of IL-2 across the different conditions, we took advantage of the fact that IL-2 from human origin is as potent a ligand for murine IL-2R as the endogenous IL-2 (Deenick et al., 2003). We could therefore control the amount of total IL-2 in the culture by using an antibody that blocked specifically secreted murine and not human IL-2 and by dispensing a fixed concentration of human IL-2.

As anticipated from the previous observation that OT-1 cells receiving strong TCR stimuli (K^b/N4) were insensitive to any co-optation from co-cultured P14 T cells, the addition of external IL-2 or inhibition of JAK had little impact on their proliferation (Figures 2C and 2D). In contrast, inhibition of MAPK and PI3K both affected the percentage of cells that divided after stimulation with Kb/N4. Addition of external IL-2 could only rescue the proliferation of cells treated with a MEK1/2 inhibitor and not with a PI3K inhibitor (Figures 2C and 2D).

In comparison to these strong TCR stimuli, intermediate TCR stimuli (K^b/T4) induced a lower percentage of cells to divide in the absence of IL-2 and the addition of external IL-2 was found to increase this percentage. Similarly to the K^b/N4 case, the impact of MEK1/2 and not of PI3K inhibition could be rescued with the addition of IL-2.

In the case of weak TCR stimuli (K^b/G4), proliferation was only observed in the presence of IL-2 (Figures 2C and 2D). In line with our results with short-term signaling assays (Figure 2B), inhibition of JAK and PI3K abrogated the effect of IL-2 whereas inhibition of MEK1/2 was insignificant in terms of cell-cycle entry. We also measured the upregulation of the IL-2Rα receptor subunit in the presence of IL-2 under PI3K inhibition (at an inhibitor dose for which entry into cell cycle was blocked; Figure S3), but not under JAK inhibition: this demonstrated that IL-2R upregulation was mediated by the JAK-STAT pathway and was largely independent of PI3K activity. Our experiments thus delineated the overlapping signaling responses downstream of TCR and IL-2R: initial TCR signals are critical to drive IL-2Rα expression, which in turn enables IL-2 responsiveness and further PI3K activation.

Such PI3K activation then acts as the integration point between the TCR and IL-2 pathways controlling the entry into cell cycle for weakly stimulated CD8+ T cells in the presence of IL-2.

A Hybrid Stochastic/Deterministic Model Recapitulates the Distribution of First Division Times and Its Modulation by IL-2

Our previous results indicate that IL-2 can modulate cells' decision to enter cell cycle through the activation of the PI3K-AKT-mTOR pathway. We found that this decision to enter the cell cycle was highly heterogeneous, even within isogenic populations of cells: after 3 days in the presence of IL-2, a fraction of weakly stimulated cells underwent up to five cell divisions (>20%) whereas others had not started to divide (Figure 2D).

To understand the origin of this divergence of cell fates—between entering the cell cycle or not (Au-Yeung et al., 2014)—and the tuning role of IL-2, we developed a quantitative model that bridges the different time scales of the events occurring during the first days following antigen encounter (Figure 3A; see Supplemental Experimental Procedures and Figure S4 for a complete definition of the model). We modeled the activation of T lymphocytes at the individual cell level by modeling the signaling responses downstream of the TCR and IL-2R. Engagement of these receptors in turn activates transcription factors that regulate the expression of cytokine, cytokine receptors, and CyclinD (a critical regulator of cell-cycle entry).

To account for the observed phenotypic variability in cell-cycle entry, we implemented a mixed deterministic/stochastic modeling framework. We reasoned that signaling responses occur on fast timescales (min) using large number of proteins (e.g., 30,000 receptors for the antigen): these could be modeled with steady-state approximations or deterministic ordinary differential equations. As far as transcriptional responses are concerned, their slow dynamics and the low copy number of mRNA (e.g., for IL-2Rα and CyclinD) necessitate a stochastic treatment. Such stochasticity generates cell-to-cell variability that may account for heterogeneity in cell-cycle entry within isogenic population of cells.

From our theoretical point of view, the modulation of cell-cycle entry by IL-2 can be best understood by considering the two "extreme" regimes:

(1) *In the absence of IL-2*, the constant presence of a strong agonist antigen (characterized by a long half-life of binding with the TCR; τ = 10 s) leads to an equilibrium distribution for IL-2Rα peaked at a finite value close to its mean value set to 10^3 copies per cell (Figures 3B and S2). For a weaker agonist (τ = 1 s), this equilibrium distribution is shifted toward smaller values. Importantly, even though its mode corresponds to null expression of IL-2Rα, indicating that the most probable number of IL-2Rα molecules per cell at any given time is zero, the tail of this distribution is long and a fraction of cells also express amounts of IL-2Rα similar to those obtained with a strong agonist (see experiments in Figure S2).

(2) Conversely, *in the absence of antigen and in the condition where the level of IL-2 is maintained constant*, the mean value of IL-2Rα reached at equilibrium depends on the constant amount of IL-2 provided. Without IL-2, the basal
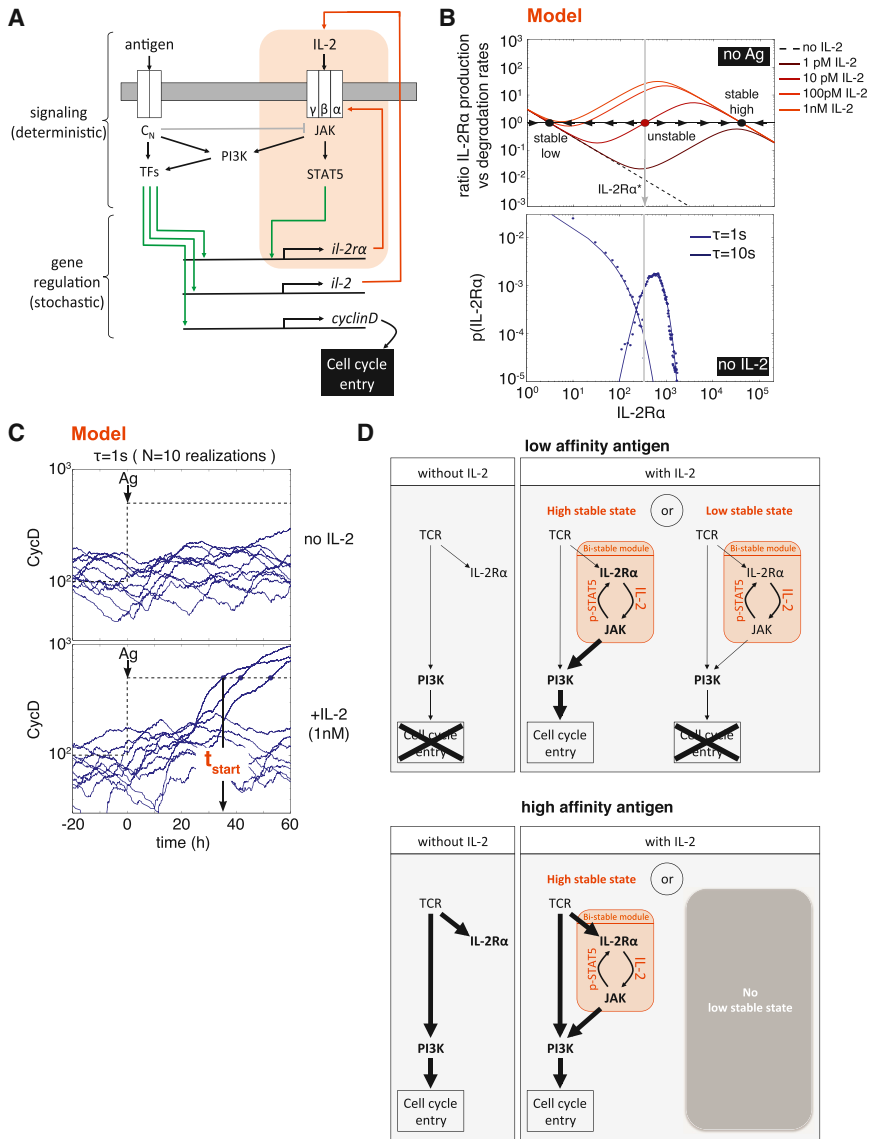
Figure 3. A Hybrid Computational Model for the Regulation of Cell Cycle Entry through the Integration of TCR and IL-2R Signals Exhibits a Bistable Behavior

(A) Schematic representation of the hybrid quantitative model for the interplay between TCR and IL-2 signaling in the regulation of cell-cycle entry. Events occurring on short timescales, such as phosphorylations, are treated as deterministic, and we assume quasi-equilibrium for the corresponding variables. Events occurring on long timescales, such as gene transcription and mRNA translation, are treated as stochastic (green arrows). For weakly TCR stimulated cells, variability in the expression of the IL-2 receptor (IL-2Rα) ensures that only a fraction of them express a sufficient amount of the receptor to efficiently trigger the (IL-2Rα+IL-2) > (pSTAT5) > (IL-2Rα) positive feedback loop (highlighted in red), leading to a (IL-2Rα)-high state and further activating PI3K and allowing the subsequent entry into the cell cycle.

(B) IL-2Rα production and degradation rate as a function of IL-2Rα in the absence of antigen (upper panel). In the presence of a constant dose of IL-2, the (IL-2Rα+IL-2) > (pSTAT5) > (IL-2Rα) positive feedback loop (highlighted in red in A) leads to the co-existence of two stable equilibrium points (high and low represented as solid black circles) separated by an intermediate unstable point (represented as a solid red circle). A cell expressing more (resp. less) IL-2Rα than this intermediate level (represented by the vertical gray line) will eventually reach the high (resp. low) stable state. We report the equilibrium distributions of IL-2Rα levels in absence of IL-2 for constant levels of two antigens with different affinities for the TCR (a weak agonist, τ = 1 s, and a strong agonist, τ = 10 s). Dots are results of the stochastic simulation, and solid lines are theoretical distributions obtained as described in Friedman et al. (2006). In the case of the weak agonist in the presence of a given dose of IL-2 and at a given time, only a fraction of cells are above the intermediate unstable IL-2Rα level (vertical gray line).

(C) Time evolution of the number of CyclinD molecules for five different cells in the case of a stimulation by a weak agonist (τ = 1 s at time t = 0, without IL-2, or in the presence of an initial dose of IL-2 (1 nM). Cell-cycle entry happens when the number of CyclinD molecules accumulated in the cell overcomes a fixed threshold (represented by the black dashed line). Time of the first division is denoted as "t$_{start}$".

(D) Simplified representation of the model behavior under different stimulatory conditions (with low/high affinity antigen in the presence or absence of IL-2). Weakly stimulated cells rely on the presence of IL-2 to activate PI3K and subsequently enter cell cycle. The presence of a bi-stable module ensures that only a fraction of weakly stimulated cells (those reaching the high stable state) enter cell cycle. For cells stimulated through their TCR with a strong agonist, PI3K is efficiently activated downstream of the TCR. Hence, additional inputs from engaged IL-2 receptors have little impact on the overall PI3K activity and on the subsequent entry into cell cycle.

rate of transcription of the *il-2rα* gene provides a unique stable equilibrium point with only a few IL-2Rα molecules per cell (Figure 3B). In the presence of a sufficient amount of IL-2, another stable equilibrium point exists with a large number of IL-2Rα molecules per cell. Given the dependency of IL-2 signaling on IL-2Rα abundance (Cotari et al., 2013), as illustrated in Figure S5, these two stable equilibrium points can coexist for an intermediate dose of IL-2 and are separated by an unstable equilibrium point for intermediate abundances (IL-2Rα* ∼300 for [IL-2] = 10

pM). Accordingly, in this particular case, a cell with an abundance of IL-2Rα greater (resp. smaller) than IL-2Rα* will eventually reach the high IL-2Rα (resp. low IL-2Rα) stable equilibrium point.

We used our model to probe the more-realistic regime when both the availability of antigen and IL-2 are dynamically regulated: at any given time, the quantity of IL-2Rα expressed by a cell and the amount of available IL-2 set a tendency to evolve toward one or the other equilibrium state. In the high-equilibrium
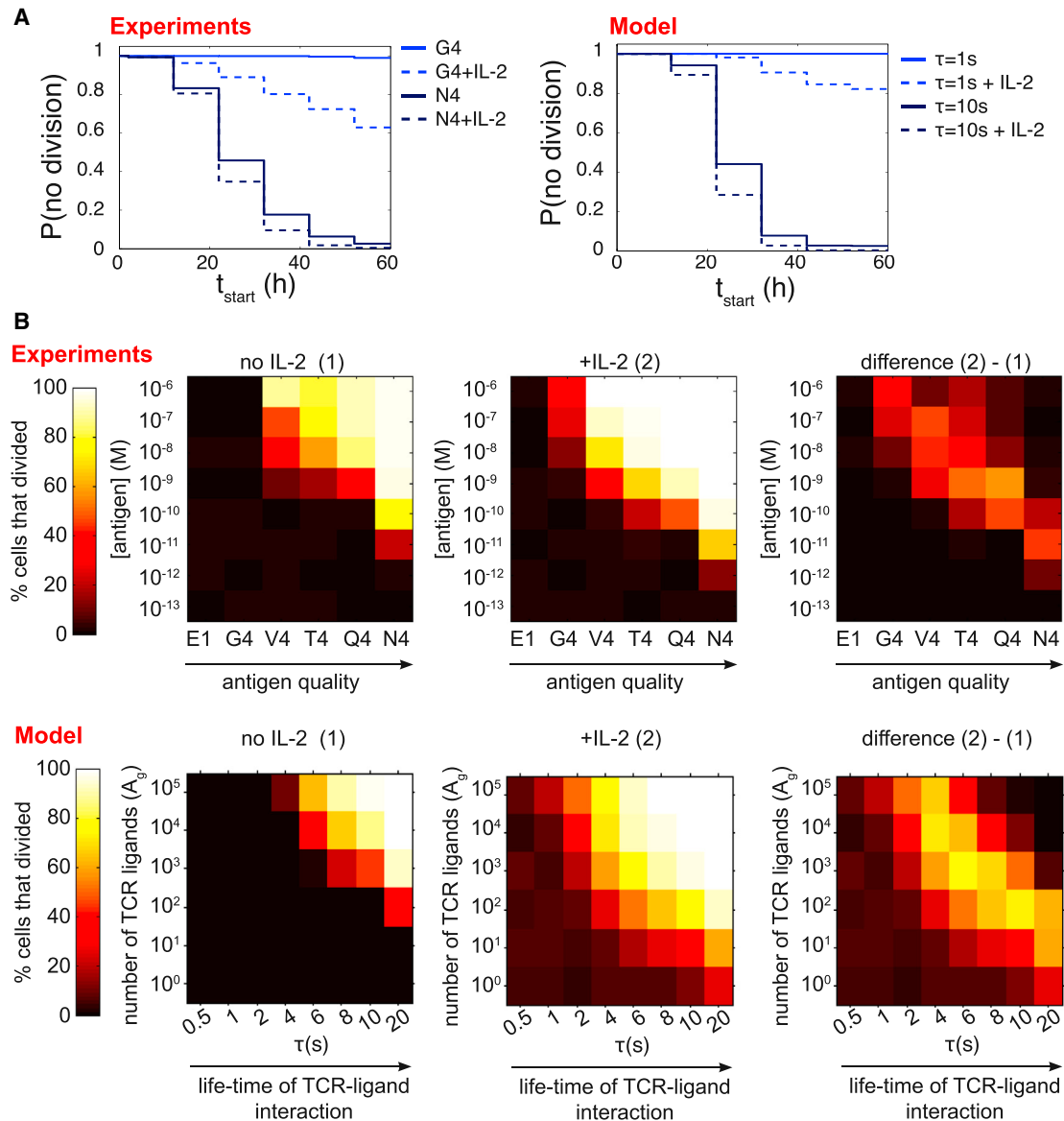
Figure 4. The Model for CD8+ T Cell Activation Recapitulates IL-2 Modulation of Cell Cycle Entry

(A) Comparison between the experimental and theoretical distributions of first division times t_{start}. Experiments: OT-1 T cells were stimulated with antigens of varied strength (Kb/N4 and Kb/G4) and cultured for 3 days in the presence of a blocking antibody against the endogenous mouse IL-2 (clone JES6-1A12) either alone or with the addition of an initial dose (1 nM) of human IL-2. The cumulative distribution of first division times was computed from the GMFI of the amine reactive dye CTV, assuming a constant doubling period of 10 hr. Model: for each condition, we simulated independently 10^3 different cells stimulated by a weak or a strong antigen (τ = 1 s or τ = 10 s) at time t = 0, without IL-2, or in the presence of an initial dose of IL-2 (1 nM).

(B) Representation of the percentage of OT-1 precursor cells that divided as a function of antigen quality and antigen quantity. Experiments: OT-1 T cells were stimulated with APCs pulsed with antigens of varied strength (from E1 to N4) at various concentrations and cultured for 3 days in the presence of a blocking antibody against the endogenous mouse IL-2 (clone JES6-1A12) either alone (condition 1: "no IL-2," left) or with the addition of an initial dose (1 nM) of human IL-2 (condition 2: "+IL-2" condition, center). The difference between these two conditions is represented on the panel on the right. Model: for each condition, we simulated independently 10^3 different cells stimulated by APCs presenting 10° to 10^5 ligands (parameter A_g) of a given affinity for the TCR (parameter τ) at time t = 0, without IL-2, or in the presence of an initial dose of IL-2 (1 nM).

state, signals transmitted through the IL-2R are at a maximum and PI3K is efficiently activated. In the case of stimulation with a weak agonist (τ = 1 s), the occasional bifurcations toward the high-equilibrium point in the presence of IL-2 allow enough PI3K activation to efficiently accumulate CyclinD molecules

and to eventually cross the threshold for cell-cycle entry (Figures 3C and 3D) as observed experimentally (Figure S2).

The proposed model reproduced accurately the experimental distribution of first division times for strong and weak agonists in the presence or absence of IL-2 (Figure 4A). For strong agonists

(τ = 10 s), PI3K activation is initially dominated by signals generated by the TCR and CyclinD is efficiently accumulated without any need for additional inputs from the IL-2R (Figure 3D). For weak agonists (τ = 1 s), initial TCR signals fail to generate enough CyclinD on their own and crossing of the CyclinD accumulation threshold necessitates PI3K activation through IL-2 signals. Our model for TCR signaling (François et al., 2013) indicates that low presentation of strong agonists results in proximal TCR signals comparable in strength to those obtained with a large quantity of weak agonists. As such, our global model for the integration of TCR and IL-2R signals predicted that IL-2 should also modulate cell-cycle entry for cells stimulated with low quantities of strong agonists and more generally with weak TCR signals. Such quantitative predictions were accurately verified experimentally by titrating the presentation of a number of peptide variants with different affinities for the OT-1 TCR, namely E1, G4, V4, T4, Q4, and N4 in ascending order, in the presence or absence of exogenous IL-2 (Figure 4B). All together, our computational model accounts for the impact of local (antigen-based) and global (IL-2-derived) cues that T cells must integrate to decide whether to enter cell cycle or not.

Inter-clonal Co-optation within a Population of T Lymphocytes Is Modulated by Cell Density, Antigen Availability, and Presence of T-reg Cells

We then derived quantitative predictions from our computational model to test how variable co-optation of weakly stimulated T cells is. Experimentally, we observed that co-optation of weakly stimulated T cells depended not only on the total quantity of IL-2 (Figure S1) available but also on the timing of IL-2 presence (Figure S1). Our model for global IL-2 accumulation predicted that the duration of IL-2 availability above a certain concentration and the amount of accumulated IL-2 depended on many parameters, including the number of initial precursors, antigen availability, and the introduction of IL-2 competitors consuming the shared resource (Figure S5). To test this prediction experimentally, we investigated how the density of co-opting P14 cells and the presence of IL-2-consuming cells (e.g., CD4+CD25+ regulatory T cells a.k.a. T-reg cells) impacted the inter-clonal co-optation of weakly stimulated T cells. We isolated T-reg cells from wild-type splenocytes and included them in our in vitro co-culture system (Figure 5A). As detailed above, we tracked the number of cell division experienced by both the co-opting P14 cells and the weakly activated OT-1 cells (Figure 5B). As expected, we observed that the co-optation of weakly activated OT-1 cells depended on the density of strongly activated P14 cells. At low cell density, we found that T-reg cells suppressed the co-optation of weakly activated OT-1 T cells as efficiently as a direct blockade of IL-2. In contrast, the suppressive action of T-reg cells was mostly lost at higher densities of co-opting cells (Figure 5C). Titrating the presentation of the strong antigen for P14 cells along with the number of P14 cells revealed that this dependency on the density of co-opting cells was not absolute. Indeed, we observed that T-reg cells could suppress the inter-clonal co-optation even at high density of co-opting cells, when these cells were stimulated with less antigen (Figures 5D and 5E). These different observations were found to be in good agreement with model predictions (Figure 5E).

Together, our theoretical and experimental results suggest an alternative role for IL-2 consumption by T-reg cells: in addition to acting on the survival and differentiation of proliferating CD8+ T cells (Kastenmuller et al., 2011; Pandiyan et al., 2007), our data suggest that competition for IL-2 is a suppressive mechanism that may also act on the initial cell-cycle entry for weakly activated CD8+ T cells. In addition to modulating the recruitment to APC (Pace et al., 2012), IL-2 deprivation could therefore constitute an alternative mechanism by which T-reg cells shape the repertoire of T cell clones and restrain the activation of low-affinity T cells.

DISCUSSION

Our study investigated how IL-2 provided by strongly activated T cells can synergize with the T-cell-intrinsic response to antigen to fine-tune overall T cell activation. Weak antigens are usually insufficient to trigger the full activation of cells through their sole engagement of the TCR. However, the overlay of multiple pathways into canonical signaling responses (e.g., ERK, PI3K phosphorylation, or NFkB activation) creates the possibility for a crosstalk between signaling responses and the cooperative tuning of T cell activation through external stimuli.

Here, we demonstrated that a mixed population of two clones of T cells indeed synergizes to drive the activation of the sub-optimal clones through sharing of IL-2. Mapping experimentally how cell decision to divide is made led us to identify PI3K activation as the key signaling response integrating TCR and IL-2R signals (Figure 2). Conventional understanding of T cell activation would dictate that IL-2 acts as a differentiating/mitogenic signal at intermediate or late timescales, after T cells are already fully committed to the activated states and ready to "read" cytokine cues to drive differentiation (Pipkin et al., 2010), to accelerate cell proliferation or to abrogate apoptosis (Hart et al., 2014). Our experiments demonstrate that blocking CD25 in the first hours of antigen activation does abrogate the synergetic effect of IL-2 even at times when key surface proteins associated with activation (e.g., CD69 and CD25) have not yet been fully upregulated (Figures 1F and 2E). Hence, one surprising result of our quantitative study is that IL-2 can act during the first hours of T cell activation and alter the threshold of antigen discrimination (Figure 3F).

We confirmed the activation status of weakly stimulated CD8+ T cells proliferating in presence of IL-2 by comparing their expression of surface markers CD44 and CD69, transcription factors Tbet and Eomes, as well as production of IL-2 and IFN-γ to that of strongly stimulated cells proliferating without external IL-2 (Figure S2). Whereas the induction of Tbet and IFN-γ were found comparable, CD44 and CD69 were less abundant and expression of the transcription factor Eomes was increased, indicating a bias toward the memory phenotype for T cells activated with weak antigens (Intlekofer et al., 2005). In agreement with observations by other groups (Catron et al., 2006; Williams et al., 2006), our results support a role for IL-2 in mediating the generation of a T cell memory pool originating from weakly stimulated T cells.

Our study highlights the relevance of quantitative models in immunology in validating the sufficiency of identified molecular mechanism to account for observed phenotypes. We built a
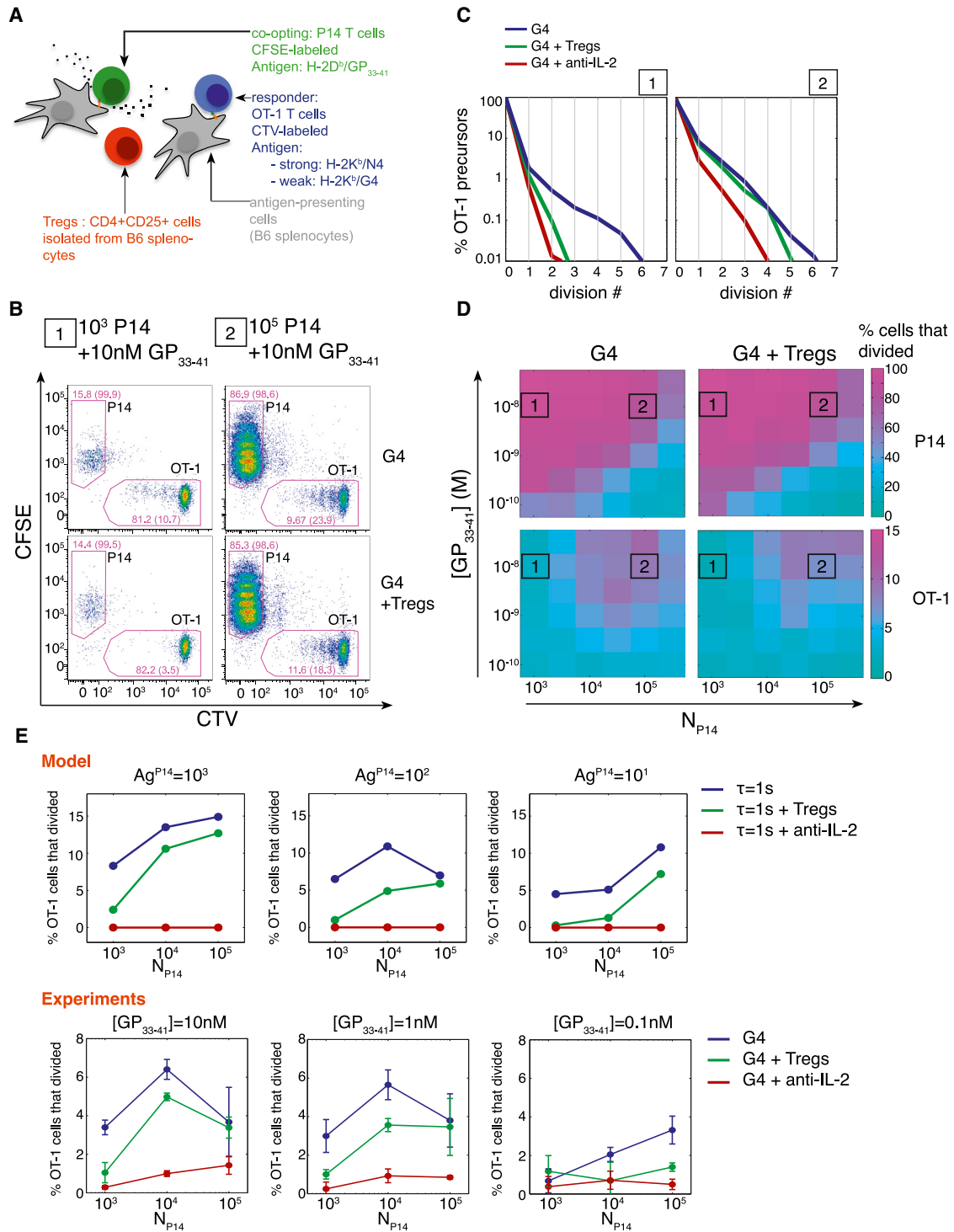
Figure 5. T-reg Cells Can Modulate IL-2-Mediated Inter-clonal Co-optation of Weak T Cell Clones

(A) CD4+CD25+ T-reg cells were added to the in vitro co-culture system introduced in Figure 1A.

(B) Representative dot plot of CFSE and CTV MFI for live CD8+ cells after 3 days of co-culture in absence or presence of T-reg cells (isolated as CD4+CD25+ from B6 splenocytes). OT-1 cells were stimulated by APCs pulsed with the weak agonist G4 (1 μM) in the presence of different quantities (condition 1, 10^3; condition 2, 10^5) of P14 cells stimulated by APCs pulsed with their cognate antigen GP_{33-41} (10 nM). Drawn gates identify P14 and OT-1 populations within live CD8+ cells, and their respective frequencies are indicated. For each population, the percentage of cells that divided at least once is also indicated in parentheses.

(legend continued on next page)

hybrid stochastic/deterministic model integrating TCR and IL-2R signals at the level of PI3K activation to control cell-cycle entry. First, we established our model for individual lymphocyte responding to cell-centered antigens and collectively shared cytokines (Figure 3). Non-linearity in signal transduction coupled to stochastic gene expression allowed to understand the source of divergence and the tuning role of IL-2 between the decisions to enter cell cycle or not. We then used our model to test how a polyclonal population of cells responds collectively, under varied stimulatory conditions such as varied precursor frequencies, varied amounts of antigen, presence, or absence of regulatory T cells (Figure 4). Such back and forth between biochemically explicit model and experimental validation is expanding our quantitative understanding of the immune system (Hart et al., 2014; Tkach et al., 2014). Future research will need to include spatio-temporal heterogeneities that are the hallmark of cytokine communication in vivo (whereas this study focused on establishing a well-mixed model that matches our experimental settings in vitro).

Through the mechanism we have put forward here, weakly self-reactive clones could be triggered into clonal expansion as a bystander effect in other immune reactions. Our results therefore highlight the importance of mechanisms regulating the concentration of inflammatory cues, for instance via consumption by T-reg cells, to prevent the development of autoimmune diseases and maintain self-tolerance.

In this study, we demonstrate how heterogeneous gene expression (in our case of IL-2Rα) can lead, albeit under the same environmental circumstances, to different cell fates. In the case of the immune system, such divergence of cell fates could help maintain the diversity of the T cell repertoire in order to cope with future unpredictable challenges. Similar behaviors exist in other systems, such as bacterial populations, where heterogeneous virulence gene expression can promote the survival of a fraction of the population against exposure to antibiotics through a bet-edging mechanism (Deris et al., 2013). These results suggest that bi-stability in the response to environmental cues could serve as a general strategy employed by biological systems to cope with changing, uncertain environments.

The long-term practical impact of our study will be in the field of immunotherapy, where expansion of the pool of T cells involved in an immune response may be a useful tool to boost immune responses. Based on our study, we posit that appropriately timed and dosed delivery of IL-2 may constitute a valuable approach to co-opt weak T cell clones into contributing to the immune response (e.g., against weakly antigenic tumors). Other manipulation of the inflammatory milieu—such as delivery of IFN-γ (Richer et al., 2013) and boosting/blocking of the regulatory T cell compartment (Boyman et al., 2006)—will need to be further explored to expand or limit the repertoire of T cell clones acquiring effector function.

Overall, our study highlights how antigen discrimination by T lymphocytes is not uniquely a cell-intrinsic property of the signaling cascades but should be considered as the integration of multiple cues, from the local, with the quality and quantity of antigens, to the global, with the dynamics of accumulation of and response to inflammatory cytokines.

EXPERIMENTAL PROCEDURES

Mice, Antibodies, and Reagents
Mice
C57BL/6N (Taconic Farms), OT-1 TCR transgenic (NIAID model number 4175; Taconic Farms) on a Rag1−/− background, and LCMV-P14 TCR transgenic mice (NIAID model number 4138; Taconic Farms) were used to prepare culture of primary lymphocytes. All mice were bred and maintained in accordance with the protocol (MSKCC no. 05-12-031) approved by the institutional animal care and use committee (IACUC) of Memorial Sloan Kettering Cancer Center.
Antigen Peptides
The LCMV-P14 TCR agonist peptide KAVYNFATM (GP$_{33-41}$) and the OT-1 TCR agonist ovalbumin peptide SIINFEKL (N4), along with its variants EIINFEKL (E1), SIIGFEKL (G4), SIIVFEKL (V4), SIITFEKL (T4), and SIIQFEKL (Q4), were obtained from Genscript.
Antibodies
Antibodies against surface molecules CD8α (clone 53–6.7) and CD25 (IL-2Rα; clone PC61) were purchased from BioLegend. Antibodies against CD44 (clone IM7) and CD69 (clone H1-2F3) were from BDBiosciences. Neutralizing antibodies against mouse IL-2 (clone JES6-1A12), mouse IL-4 (clone 11B11), and CD25 (clone PC61.5) were purchased from eBioscience and BioXCell.

Primary antibodies against phospho species phospho-p42/p44 MAPK (pp-ERK; Thr202/Tyr204; clone E10), phospho-S6 ribosomal protein (p-S6; Ser235/236; clone D57.2.2E) and phospho-STAT5 (p-STAT5; Tyr694; clone C11C5) were purchased from Cell Signaling Technology. Secondary rat antibody against mouse IgG-APC was purchased from Jackson ImmunoResearch Laboratories. Secondary goat antibody against rabbit IgG F(ab')2-PeCy7 was purchased from Santa Cruz Biotechnology.
Small-Molecule Inhibitors
Chemical inhibitors targeting JAK (JAKi; AZD1480), MEK1/2 (MEKi; PD 0325901), and PI3K (PI3Ki; LY294002) were purchased from Selleckchem.
Other Reagents
The viability dye (Live/Dead Fixable Yellow) and amine reactive dyes CFSE (5(6)-carboxyfluorescein diacetate N-succinimidyl ester) and CTV (Cell Trace Violet) were purchased from Life Technologies. Recombinant human IL-2

(C) Distributions of the number of cell divisions per OT-1 precursor cells after 3 days in the in vitro co-culture system for the co-culture conditions 1 and 2 presented in (B) in the presence or absence of T-reg cells or IL-2 blockade. At low density of co-opting P14 cells, T-reg cells suppress the co-optation of weakly stimulated OT-1 cells as efficiently as a direct block of IL-2, and this effect vanishes as the density of co-opting cells increases.

(D) Representation of the percentage of P14 and OT-1 precursors cells that divided, in the presence or absence of T-reg cells, as a function of the density of co-opting P14 cells and the concentration of their cognate antigen GP$_{33-41}$ used to pulse the corresponding APCs. The conditions 1 and 2 referenced in (B) and (C) are indicated.

(E) The hybrid model correctly predicts the dependency of the suppression of the inter-clonal co-optation by T-reg cells as a function of the co-opting cell density. We report the percentage of OT-1 precursor cells that divided as a function of the density of co-opting P14 cells for different quantities of their cognate antigen GP$_{33-41}$ and in the presence or absence of T-reg cells and IL-2 blockade. Model: OT-1, P14, and T-reg cells were simulated simultaneously using replicates of the model presented in Figure 3. OT-1 cells were stimulated by a weak agonist (τ = 1 s). In the case of P14 cells, the cognate antigen was taken as a strong agonist with parameter τ = 10 s. For T-reg cells, no specific antigen was introduced, but we considered a high basal transcription rate of the IL-2Rα gene to generate the high abundance (set here to 10^3 copies per cell in the basal state) of IL-2Rα characteristic of this population. Simulation results shown were obtained with 10^4 T-reg cells per condition. For each condition, the percentage of cells that divided was estimated from 10^3 independent simulations. Experiments: cells were co-cultured for 3 days as in (B)–(D). Error bars represent mean ± SD for two replicates; the results are representative of n ≥ 3 independent experiments.

and mouse IL-2, IL-4, IL-6, IL-7, IL-9, IL-15, IL-21, and IFN-γ were obtained from eBioscience. All cell cultures were prepared in complete RPMI prepared by the MSKCC core media preparation facility (this medium contained RPMI-1640 augmented with 10% fetal bovine serum, 10 μg/ml penicillin/strep, 2 mM glutamine, 10 mM HEPES [pH 7.0], 1 mM sodium pyruvate, 0.1 mM non-essential amino acids, and 50 μM β-mercaptoethanol). For flow cytometry analysis, FACS buffer consisted of 10% fetal bovine serum (MSKCC tissue culture core facility) and 0.1% sodium azide in PBS.

Cell Cultures

For signaling assays, OT-1 T cell cultures were prepared as follows. Irradiated (3,000 RAD) C57BL/6N (B6) splenocytes were pulsed for 2 hr with SIINFEKL (N4) peptide, washed once, and used as APCs. OT-1 cells were harvested from spleen and mixed with N4-pulsed B6 splenocytes in complete RPMI. After 2 days, cells were expanded by 2-fold dilution into complete medium with 1 nM IL-2. After 4 days, the cells were again expanded by 2-fold dilution into complete medium with IL-2. After 1 more day of culture, cells were harvested and spun through a 1.09-density Ficoll-Paque Plus gradient (GE Healthcare) to remove dead cells. Live cells were recovered, washed twice in complete medium, and resuspended at 1 million/ml in complete medium with 1 nM IL-2. Cells were used for experiments between 6 and 8 days after primary stimulation.

Cytokine-Signaling Assay

Live cells were purified from collected cells by separation on a Ficoll gradient. In order to strip surface receptors from bound cytokines, cells were resuspended in a glycine buffer (0.1 M; pH 4.0) for 1 min on ice, washed twice in complete RPMI, and allowed to rest for at least 30 min at 37°C. Cells were pre-incubated with small-molecule inhibitors for 15 min before stimulation. Inhibitor concentrations were maintained at the same level during stimulation. Cells were stimulated with 1 nM recombinant mouse IL-2 in complete RPMI and placed on a water bath at 37°C for 15 min. Cells were then directly fixed for 10 min on ice in 2% paraformaldehyde followed by permeabilization on ice in 90% methanol for at least 10 min. Cells were then washed twice in FACS buffer and stained with antibodies specific for different phosphorylated species, followed by incubation with labeled secondary antibody and conjugated antibodies specific for surface markers (CD8α and IL-2Rα).

Proliferation Assays

For proliferation assays, irradiated (3,000 RAD) C57BL/6 splenocytes were used as APCs. APCs were pulsed for 2 hr with a given peptide before being washed extensively in complete RPMI. Responder OT-1 and P14 cells were harvested from spleen and stained with 2.5 μM of CTV and CFSE, respectively. CD8α+ P14 cells were then isolated using antibody-coupled magnetic beads (Miltenyi Biotec) and the percentage of CD8α+ OT-1 and P14 cells was measured on a LSRII instrument (BD Bioscience). Unless otherwise indicated, for a given responder cell type, 10^5 CD8α+ responder cells were stimulated with 2.5×10^5 APCs pulsed with 1 μM of the corresponding peptide per well of a 96 V bottom plate (Thermo Scientific). In the case where T-reg cells are present, 10^5 CD4+CD25+ cells isolated from C57BL/6N splenocytes using magnetic beads (Miltenyi Biotec) were added. Indicated cytokines (1 nM unless otherwise indicated), blocking antibodies (4 μg/ml), and chemical inhibitors were then added to reach a final volume of 200 μl per well. Contacts between T cells and APCs were synchronized using a quick centrifugal spin (10 s at 450 g) before incubation at 37°C. After the indicated incubation period, cells were washed in PBS and stained with a viability dye (Live/Dead Yellow). Cells were then resuspended in FACS buffer and stained for surface markers. Fluorescence was then acquired on a LSRII instrument (BD Bioscience).

Quantification of Precursor Cell Number

P14 and OT-1 cells were identified among live CD8α+ cells based on the GMFI of CFSE and CTV using the FlowJo software. The number of cell divisions experienced by a cell of a given type was obtained from the dilution profile of the corresponding dye. The number of cells having experienced *k* divisions until the time of observation t_{obs}, denoted N_k, was obtained using gates defined around identified peaks in the distribution of the corresponding dye. Assuming a uniform and constant doubling period T, the number of precursor cells that divided k times was estimated as $NP_k = N_k/2^k$. The corresponding time of first division was then computed as $t_{start} = t_{obs} - k*T$. At the time of observation t_{obs}, the percentage of cells that divided at least once is given by $(\Sigma_{k > 0} NP_k)/(\Sigma_k NP_k)$.

REFERENCES

Altan-Bonnet, G., and Germain, R.N. (2005). Modeling T cell antigen discrimination based on feedback control of digital ERK responses. PLoS Biol. 3, e356.

Au-Yeung, B.B., Zikherman, J., Mueller, J.L., Ashouri, J.F., Matloubian, M., Cheng, D.A., Chen, Y., Shokat, K.M., and Weiss, A. (2014). A sharp T-cell antigen receptor signaling threshold for T-cell proliferation. Proc. Natl. Acad. Sci. USA 111, E3679–E3688.

Boyman, O., Kovar, M., Rubinstein, M.P., Surh, C.D., and Sprent, J. (2006). Selective stimulation of T cell subsets with antibody-cytokine immune complexes. Science 311, 1924–1927.

Brennan, P., Babbage, J.W., Thomas, G., and Cantrell, D. (1999). p70(s6k) integrates phosphatidylinositol 3-kinase and rapamycin-regulated signals for E2F regulation in T lymphocytes. Mol. Cell. Biol. 19, 4729–4738.

Buchholz, V.R., Flossdorf, M., Hensel, I., Kretschmer, L., Weissbrich, B., Gräf, P., Verschoor, A., Schiemann, M., Höfer, T., and Busch, D.H. (2013). Disparate individual fates compose robust CD8+ T cell immunity. Science 340, 630–635.

Busse, D., de la Rosa, M., Hobiger, K., Thurley, K., Flossdorf, M., Scheffold, A., and Höfer, T. (2010). Competing feedback loops shape IL-2 signaling between helper and regulatory T lymphocytes in cellular microenvironments. Proc. Natl. Acad. Sci. USA 107, 3058–3063.

Catron, D.M., Rusch, L.K., Hataye, J., Itano, A.A., and Jenkins, M.K. (2006). CD4+ T cells that enter the draining lymph nodes after antigen injection participate in the primary response and become central-memory cells. J. Exp. Med. 203, 1045–1054.

Cho, J.H., Kim, H.O., Kim, K.S., Yang, D.H., Surh, C.D., and Sprent, J. (2013). Unique features of naive CD8+ T cell activation by IL-2. J. Immunol. 191, 5559–5573.

Cotari, J.W., Voisinne, G., Dar, O.E., Karabacak, V., and Altan-Bonnet, G. (2013). Cell-to-cell variability analysis dissects the plasticity of signaling of common γ chain cytokines in T cells. Sci. Signal. 6, ra17.

Deenick, E.K., Gett, A.V., and Hodgkin, P.D. (2003). Stochastic model of T cell proliferation: a calculus revealing IL-2 regulation of precursor frequencies, cell cycle time, and survival. J. Immunol. 170, 4963–4972.

Deris, J.B., Kim, M., Zhang, Z., Okano, H., Hermsen, R., Groisman, A., and Hwa, T. (2013). The innate growth bistability and fitness landscapes of antibiotic-resistant bacteria. Science 342, 1237435.

Feinerman, O., Germain, R.N., and Altan-Bonnet, G. (2008a). Quantitative challenges in understanding ligand discrimination by alphabeta T cells. Mol. Immunol. 45, 619–631.

Feinerman, O., Veiga, J., Dorfman, J.R., Germain, R.N., and Altan-Bonnet, G. (2008b). Variability and robustness in T cell activation from regulated heterogeneity in protein levels. Science *321*, 1081–1084.

Feinerman, O., Jentsch, G., Tkach, K.E., Coward, J.W., Hathorn, M.M., Sneddon, M.W., Emonet, T., Smith, K.A., and Altan-Bonnet, G. (2010). Single-cell quantification of IL-2 response by effector and regulatory T cells reveals critical plasticity in immune response. Mol. Syst. Biol. *6*, 437.

François, P., Voisinne, G., Siggia, E.D., Altan-Bonnet, G., and Vergassola, M. (2013). Phenotypic model for early T-cell activation displaying sensitivity, specificity, and antagonism. Proc. Natl. Acad. Sci. USA *110*, E888–E897.

Friedman, N., Cai, L., and Xie, X.S. (2006). Linking stochastic dynamics to population distribution: an analytical framework of gene expression. Phys. Rev. Lett. *97*, 168302.

Gerlach, C., Rohr, J.C., Perié, L., van Rooij, N., van Heijst, J.W., Velds, A., Urbanus, J., Naik, S.H., Jacobs, H., Beltman, J.B., et al. (2013). Heterogeneous differentiation patterns of individual CD8+ T cells. Science *340*, 635–639.

Hart, Y., Reich-Zeliger, S., Antebi, Y.E., Zaretsky, I., Mayo, A.E., Alon, U., and Friedman, N. (2014). Paradoxical signaling by a secreted molecule leads to homeostasis of cell levels. Cell *158*, 1022–1032.

Houghton, A.N., and Guevara-Patiño, J.A. (2004). Immune recognition of self in immunity against cancer. J. Clin. Invest. *114*, 468–471.

Huppa, J.B., Axmann, M., Mörtelmaier, M.A., Lillemeier, B.F., Newell, E.W., Brameshuber, M., Klein, L.O., Schütz, G.J., and Davis, M.M. (2010). TCR-peptide-MHC interactions in situ show accelerated kinetics and increased affinity. Nature *463*, 963–967.

Intlekofer, A.M., Takemoto, N., Wherry, E.J., Longworth, S.A., Northrup, J.T., Palanivel, V.R., Mullen, A.C., Gasink, C.R., Kaech, S.M., Miller, J.D., et al. (2005). Effector and memory CD8+ T cell fate coupled by T-bet and eomesodermin. Nat. Immunol. *6*, 1236–1244.

Kastenmuller, W., Gasteiger, G., Subramanian, N., Sparwasser, T., Busch, D.H., Belkaid, Y., Drexler, I., and Germain, R.N. (2011). Regulatory T cells selectively control CD8+ T cell effector pool size via IL-2 restriction. J. Immunol. *187*, 3186–3197.

Liu, B., Chen, W., Evavold, B.D., and Zhu, C. (2014). Accumulation of dynamic catch bonds between TCR and agonist peptide-MHC triggers T cell signaling. Cell *157*, 357–368.

McKeithan, T.W. (1995). Kinetic proofreading in T-cell receptor signal transduction. Proc. Natl. Acad. Sci. USA *92*, 5042–5046.

McNally, A., Hill, G.R., Sparwasser, T., Thomas, R., and Steptoe, R.J. (2011). CD4+CD25+ regulatory T cells control CD8+ T-cell effector differentiation by modulating IL-2 homeostasis. Proc. Natl. Acad. Sci. USA *108*, 7529–7534.

Pace, L., Tempez, A., Arnold-Schrauf, C., Lemaitre, F., Bousso, P., Fetler, L., Sparwasser, T., and Amigorena, S. (2012). Regulatory T cells increase the avidity of primary CD8+ T cell responses and promote memory. Science *338*, 532–536.

Pandiyan, P., Zheng, L., Ishihara, S., Reed, J., and Lenardo, M.J. (2007). CD4+CD25+Foxp3+ regulatory T cells induce cytokine deprivation-mediated apoptosis of effector CD4+ T cells. Nat. Immunol. *8*, 1353–1362.

Pipkin, M.E., Sacks, J.A., Cruz-Guilloty, F., Lichtenheld, M.G., Bevan, M.J., and Rao, A. (2010). Interleukin-2 and inflammation induce distinct transcriptional programs that promote the differentiation of effector cytolytic T cells. Immunity *32*, 79–90.

Qi, S.Y., Groves, J.T., and Chakraborty, A.K. (2001). Synaptic pattern formation during cellular recognition. Proc. Natl. Acad. Sci. USA *98*, 6548–6553.

Richer, M.J., Nolz, J.C., and Harty, J.T. (2013). Pathogen-specific inflammatory milieux tune the antigen sensitivity of CD8(+) T cells by enhancing T cell receptor signaling. Immunity *38*, 140–152.

Schulz, E.G., Mariani, L., Radbruch, A., and Höfer, T. (2009). Sequential polarization and imprinting of type 1 T helper lymphocytes by interferon-gamma and interleukin-12. Immunity *30*, 673–683.

Slifka, M.K., and Whitton, J.L. (2001). Functional avidity maturation of CD8(+) T cells without selection of higher affinity TCR. Nat. Immunol. *2*, 711–717.

Stepanek, O., Prabhakar, A.S., Osswald, C., King, C.G., Bulek, A., Naeher, D., Beaufils-Hugot, M., Abanto, M.L., Galati, V., Hausmann, B., et al. (2014). Coreceptor scanning by the T cell receptor provides a mechanism for T cell tolerance. Cell *159*, 333–345.

Tkach, K.E., Barik, D., Voisinne, G., Malandro, N., Hathorn, M.M., Cotari, J.W., Vogel, R., Merghoub, T., Wolchok, J., Krichevsky, O., and Altan-Bonnet, G. (2014). T cells translate individual, quantal activation into collective, analog cytokine responses via time-integrated feedbacks. eLife *3*, e01944.

Wang, L., Gout, I., and Proud, C.G. (2001). Cross-talk between the ERK and p70 S6 kinase (S6K) signaling pathways. MEK-dependent activation of S6K2 in cardiomyocytes. J. Biol. Chem. *276*, 32670–32677.

Williams, M.A., Tyznik, A.J., and Bevan, M.J. (2006). Interleukin-2 signals during priming are required for secondary expansion of CD8+ memory T cells. Nature *441*, 890–893.

Zehn, D., Lee, S.Y., and Bevan, M.J. (2009). Complete but curtailed T-cell response to very low-affinity antigen. Nature *458*, 211–214.